DOI:
10.1109/ACCESS.2017.2684542

Document Version
Publisher's PDF, also known as Version of record

IEEE Access
Multidisciplinary | Rapid Review | Open Access Journal

Received February 1, 2017, accepted March 15, 2017, date of publication May 8, 2017, date of current version June 7, 2017.

Digital Object Identifier 10.1109/ACCESS.2017.2684542

Full-Duplex Small Cells for Next Generation Heterogeneous Cellular Networks: A Case Study of Outage and Rate Coverage Analysis

MHD OMAR AL-KADRI[1], (Student Member, IEEE), YANSHA DENG[1], (Member, IEEE), ADNAN AIJAZ[2], (Member, IEEE), AND ARUMUGAM NALLANATHAN[1], (Fellow, IEEE)

[1]Department of Informatics, King's College London, London WC2R 2LS, U.K.
[2]Telecommunications Research Laboratory, Toshiba Research Europe Ltd., Bristol BS1 4ND, U.K.

Corresponding author: Mhd Omar Al-Kadri (mhd_omar.alkadri@kcl.ac.uk)

This work was supported by the U.K. Engineering and Physical Sciences Research Council under Grant EP/M016145/1.

ABSTRACT Full-duplex (FD) technology is currently under consideration for adoption in a range of legacy communications standards due to its attractive features. On the other hand, cellular networks are becoming increasingly heterogeneous as operators deploy a mix of macrocells and small cells. With growing tendency toward network densification, small cells are expected to play a key role in realizing the envisioned capacity objectives of emerging 5G cellular networks. From a practical perspective, small cells provide an ideal platform for deploying FD technology in cellular networks due to its lower transmit power and lower cost for implementation compared with the macrocell counterpart. Motivated by these developments, in this paper, we analyze a two-tier heterogeneous cellular network, wherein the first tier comprises half-duplex macrobase stations and the second tier consists of the FD small cells. Through a stochastic geometry approach, we characterize and derive the closed-form expressions for the outage probability and the rate coverage. Our analysis explicitly accounts for the spatial density, the self-interference cancellation capabilities, and the interference coordination based on enhanced inter-cell interference coordination techniques. Performance evaluation investigates the impact of different parameters on the outage probability and the rate coverage in various scenarios.

INDEX TERMS Full-duplex, enhanced inter-cell interference coordination, heterogeneous cellular networks, outage probability, rate coverage.

I. INTRODUCTION

In half-duplex (HD) wireless communications systems, bi-directional communications between a pair of nodes is achieved with either frequency division duplexing (FDD) or time division duplexing (TDD). The former technique employs different frequency bands for the uplink (UL) and downlink (DL), whereas, in the latter technique, a single channel is shared in the time domain for both UL and DL. Such techniques however are not suitable to fulfil the envisioned requirements of next generation wireless systems [1]. Historically, simultaneous transmission and reception in wireless communications was deemed infeasible in practice due to the so called self-interference (SI), which is the interference generated by the transmitter of a radio on its own receiver. Recent developments in SI cancellation techniques [2]–[6] have led to the practical realization of FD radios. The feasibility of single-array FD transceivers has been presented in [7] and [8]. FD technology has a number of attractive features e.g., it can potentially double (theoretically) the ergodic capacity [9], [10], reduce the feedback delay [11], decrease the end-to-end delay [12], improve the network secrecy [13] and increase the efficiency of network protocols (e.g., medium access control [14]).

On the other hand, small cells are gaining increasing popularity in the next generation cellular systems. Small cells provide an easy and cost-efficient deployment solution for capacity and coverage improvements over the conventional macro-centric networks [15], [16]. The low-powered nature of small cells make them the ideal candidate for FD deployment considering that the self-interference (SI) is more manageable compared to the conventional high-power macro counterparts. This inspires and motivates the investigation for the feasibility and performance gains of FD small cells underlay heterogeneous cellular networks (HCNs).

An important issue for HCNs is the inter-cell interference, which arises due to the dense unplanned deployments of small cells, loud neighbors, and the closed subscriber group access. To mitigate this interference, 3GPP has recently standardized the *enhanced Inter-Cell Interference Coordination* (eICIC) technique in Release 10 [17]. eICIC provides interference cancellation techniques in time, frequency, and power control domains. When the subframes of macro cells and small cells are aligned, their control and data channel overlap with each other. Therefore, eICIC mitigates the interference on the control channel of small cells through *Almost Blank Subframes* (ABS) at small cells. During ABS, the macro BSs only transmits control channels and cell-specific reference signals, no user data would be transmitted, and it is transmitted using reduced power. This allows small cell BSs to schedule the associated users without interference from the macro BSs.

A. RELATED WORK

Recent studies on modeling and analysis of HCNs heavily rely on stochastic geometry framework [18]–[21]. Using these tools, comprehensive modeling and analysis of legacy HCNs has been carried out in [22]–[25]. In [26], the authors have presented the outage probability, the average ergodic rate, and the minimum average user throughput for a downlink HD multi-tier HCNs. They have concluded that neither the number of BSs nor the tiers affect outage probability or average ergodic rate in an interference-limited full-loaded HCNs with unbiased cell association. These conclusions, however, may not hold in environments which are prone to higher interference, like HCNs comprising FD nodes.

FD-enabled wireless networks have been attracting growing interest, recently [27]. In [28], the authors have derived the expression for the throughput of hybrid duplex heterogeneous networks composed of multi-tier networks, with access points (APs) operating either in bi-directional FD mode or downlink HD mode in each tier. The authors have concluded that having tiers with hybrid duplex BSs degrades the performance, while higher throughput was achieved when each tier operates in the same duplex, either HD or FD rather than a mixture of both. This motivates further research on two-tier HCNs with FD small cells and HD macrocells, instead of considering hybrid scenarios. In [29], the authors have derived the downlink rate coverage probability of a user in a single-tier FD small cell network with massive MIMO wireless backhauls. In [30], the authors have introduced an FD-assisted cross-tier inter-cell interference (ICI) mitigation scheme called fICIC, which operates on small cells compared to the standardized eICIC that operates on the macrocells. Such a change may lead to modifications on the current backhaul affecting feasibility of application. This motivates further investigation on the application of eICIC on FD-enabled HCNs to avoid legacy network modifications. In [31], the authors consider a hybrid scenario where all BSs operate in FD mode. They derived a closed-form expression for the critical value of the self-interference attenuation power, which is required for the FD users to outperform HD users. In [32], the authors have considered a single tier mixed small cell network, where BSs operate in either HD or FD, with all users operating in HD. The effect of FD cells on the performance of the mixed system was presented, however, inter-cell interference coordination was not considered and only single tier was investigated.

B. CONTRIBUTIONS AND OUTLINE

Different from the aforementioned studies, our objective in this paper is to model and analyze an interference-coordinated two-tier HCN with FD small cells. The key contributions of this paper can be summarized as follows.

- We formulate a tractable model for the interference coordinated two-tier HCN with FD small cells, wherein tier 1 comprises legacy HD macrocells and tier 2 consists of FD small cells. By explicitly accounting for spatial distribution of base stations, self-interference, transmit power, cell association, uplink power control and ABS factor, we provide signal-to-interference-plus-noise ratio (SINR) expressions for users in the corresponding two tiers. Specifically, the underlying model captures the DL scenario for tier 1 and both UL and DL scenarios for tier 2, since tier 1 and tier 2 operate in HD and FD mode, respectively.
- Based on the system model for two-tier HCN with FD small cells, we derive closed-form expressions for outage probability of different tiers. The final expressions explicitly account for interference coordination.
- We adopt the notion of rate coverage from [33], and derive closed-form expressions for the corresponding two tiers.
- We conduct a comprehensive performance evaluation through numerical as well as simulation studies. We investigate the impact of various design parameters on network performance in various scenarios.

The rest of the paper is organized as follows. Section II provides the system model. In Section III, we analyze the outage probability of two-tier HCNs with FD small cells. This is followed by rate coverage analysis in section IV. Numerical and simulation results are given in Section V. Finally, the paper is concluded in Section VI.

II. SYSTEM MODEL

Frequently used notations and symbols have been summarized in Table 1. We consider a two-tier HCNs, where tier 1 comprises macro BSs operating in HD mode, and tier 2 consists of small cells operating in FD mode, as illustrated in Fig. 1. Both tiers are spatially distributed in $\mathbb{R}^2$ following homogeneous Poisson point processes (HPPPs) Φ_{S_1} and Φ_{S_2}, with intensities λ_{S_1} and λ_{S_2}, respectively, to represent the spatial distribution of BSs and small cells. All users operate in HD mode. The UL small cell users are spatially located in $\mathbb{R}^2$ following the HPPP Φ_{U_2}, with intensity λ_{u_2}, to represent the independent spatial distribution of the small cell users. Assuming that the intensity of DL users is high enough, and each user has data ready for transmission, such that

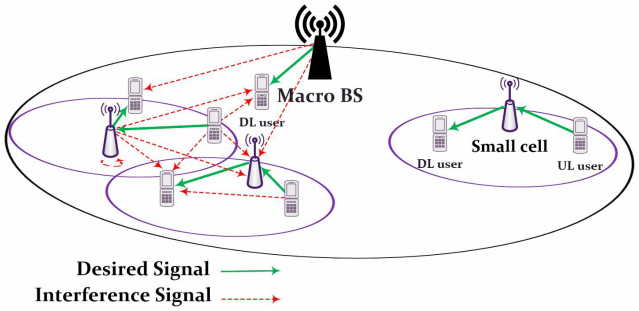

FIGURE 1. Example cells of the system model, where macro BS operates in HD mode and small cells operate in FD mode.

saturated traffic conditions hold. We also assume that each small cell BS serves single active uplink user and single downlink user per channel, and each macrocell BS serves single active downlink user per channel. This assumption is justified due to the conclusions in [28], that the highest network performance is achieved when each tier in the network operates in the same duplex, rather than having hybrid tiers. We assume that the UL users share the macro DL frequency to minimize the interference on the DL users, considering that the density of small cells is usually significantly higher than the density of macrocells. The full frequency reuse scenario is assumed, such that all the cells use the same frequency band. We assume that the channel coefficients are invariant in each block and vary between different blocks. Moreover, we assume that the channel $h_{i,j}$ between any pair of nodes i and j is impaired by Rayleigh fading, and the path loss is assumed to be inversely proportional to distance with the path loss exponent α.

We assume that the FD small cells are equipped with a single antenna and achieve FD capability through the techniques mentioned in [7] and [8]. A node in FD mode receives interference from its transmitted signal, and performs SI interference cancellation. Since the amount of SI depends on the transmission power at the receiver P_{S_2}, we define the residual self-interference (RSI) power after performing the SI cancellation as [28], [34], [35],

$$RSI = P_{S_2} H_{SI}, \tag{1}$$

where $H_{SI} = |h_{SI}|^2$ is the RSI channel gain of the small cell BS, and indicates the SI cancellation capability of that BS, where h_{SI} is the SI channel of the BS. Note that $RSI = 0$ denotes perfect cancellation capability.

The residual self-interfering channel gain H_{SI} in (1) needs to be characterized based on the applied SI cancellation algorithm. Here, we consider the digital-domain cancellation, where h_{SI} can be presented as $h_{SI} = h_{SI_c} - \hat{h}_{SI_c}$ where h_{SI_c} and $\hat{h}_{SI_c}$ are the self-interfering channel and its estimate as the self-interference is subtracted using the estimate [28], [34]–[36], which allows H_{SI} to be modeled as a constant value, such that $H_{SI} = \sigma_e^2$ for the estimation error variance σ_e^2 [28], [34], [36]. Other SI cancellation algorithms, such as analogue domain algorithms [2], [37], [38] or propagation domain algorithms [35], [39], [40] will make the modeling of H_{SI} challenging. Therefore, in our analysis, we consider H_{SI} to be a constant value. Please note that the analysis can still be easily extended to the case of random H_{SI} within our framework. For instance, once the probability density function (PDF) of H_{SI} is available for a certain SI cancellation algorithm, by averaging the analytic results presented in this paper, over the distribution of H_{SI}, the results for the random H_{SI} can be derived.

TABLE 1. Frequently used notations.

Notation	Definition
Φ_{S_x}	HPPP of base stations in tier x
Φ_{U_x}	HPPP of users in tier x
λ_{S_x}	Spatial density of base stations in tier x
λ_{u_x}	Spatial density of users in tier x
S_x	Base station of tier $x \in (1,2)$
S_x^*	Associated BS of tier $x \in (1,2)$
u_x	Users of tier $x \in (1,2)$
u_x^0	The user at origin of tier $x \in (1,2)$
RSI	Residual self-interference
P_{y_x}	Transmission power of $y \in (S,u)$ of tier $x \in (1,2)$
$h_{a,b}$	Small scale fading channel coefficient between a and b
$R_{a,b}$	Distance between a and b
$\alpha_{a,b}$	Pathloss exponent between a and b
I_y^Z	Interferences caused by $y \in (S,u)$ in $Z \in (UL,DL)$
N_0	Additive Gaussian noise
$\mathcal{A}_{S_x}$	Users association probability with BS of tier $x \in (1,2)$

We consider the maximum received power cell association rule in the downlink transmission of HCNs, adopting the flexible cell association without biasing [26]. In our case, the association probability $\mathcal{A}$ for the macrocells and the small cells can according to [26] be expressed by

$$\mathcal{A}_{S_1} = 1 - \mathcal{A}_{S_2} = 1 - \left(1 + \frac{\lambda_{S_1}}{\lambda_{S_2}} \left(\frac{P_{S_1}}{P_{S_2}}\right)^{2/\alpha_2}\right)^{-1}. \tag{2}$$

and

$$\mathcal{A}_{S_2} = \mathbb{P}\left(P_{S_2}^r > P_{S_1}^r\right) = \left(1 + \frac{\lambda_{S_1}}{\lambda_{S_2}} \left(\frac{P_{S_1}}{P_{S_2}}\right)^{2/\alpha_1}\right)^{-1}, \tag{3}$$

respectively, In (2) and (3), $P_{S_1}^r$ and $P_{S_2}^r$ are the received power at the associating user from the macrocell and small cell BSs, respectively. Moreover, α_1 and α_2 are the path loss exponents of macrocells and small cells, respectively.

In this paper, we assume that the HCNs employs eICIC technique for interference mitigation due to it's wide usage and popularity, with ABS transmission factor of ρ defined as the ratio of ABS transmitted over the total transmitted frames.

A. DOWNLINK SINR OF MACROCELL USER

For a typical macrocell downlink user located at the origin u_1^0, associated with its serving macrocell BS S_1^*, the SINR is expressed as

$$SINR_{u_1}^{DL} = \frac{P_{S_1} |h_{S_1^*,u_1^0}|^2 R_{S_1^*,u_1^0}{}^{-\alpha_1}}{I_{u_2}^{UL} + I_{S_2} + I_{S_1}^{DL} + N_0}, \tag{4}$$

where

$$I_{u_2}^{UL} = \sum_{u_2 \in \Phi_{U_2}} P_{u_2} |h_{u_2,u_1^0}|^2 R_{u_2,u_1^0}{}^{-\alpha_2},$$
$$I_{S_2} = \sum_{S_2 \in \Phi_{S_2}} P_{S_2} |h_{S_2,u_1^0}|^2 R_{S_2,u_1^0}{}^{-\alpha_2},$$
$$I_{S_1}^{DL} = \sum_{S_1 \in \Phi_{S_1} \setminus S_1^*} P_{S_1} |h_{S_1,u_1^0}|^2 R_{S_1,u_1^0}{}^{-\alpha_1}.$$

given $I_{u_2}^{UL}$ is the interference from small cell uplink users, I_{S_2} is the interference from small cell BSs and $I_{S_1}^{DL}$ is the interference from other macrocell BSs.

In (4), P_{u_2} is the transmit power of UL user associated with small cell, $h_{S_1^*,u_1^0}$, h_{u_2,u_1^0}, h_{S_2,u_1^0}, and h_{S_1,u_1^0} denote the small scale fading channel coefficient for the channels of the typical downlink user and its serving macrocell BS, small cell users, small cell BSs and other non-associated macrocell BSs, respectively. Moreover, $R_{S_1^*,u_1^0}$, R_{u_2,u_1^0}, R_{S_2,u_1^0}, and R_{S_1,u_1^0} denote the distances between the typical downlink macrocell user and its associated macrocell BS, small cell users, small cell BSs, and other interfering macrocell BSs, respectively.

B. DOWNLINK SINR OF SMALL CELL USER

For a typical small cell downlink user located at the origin u_2^0, associated with its serving small cell BS S_2^*, the SINR expression is given by

$$SINR_{u_2}^{DL} = \frac{P_{S_2} |h_{S_2^*,u_2^0}|^2 R_{S_2^*,u_2^0}{}^{-\alpha_2}}{I_{u_2}^{UL} + I_{S_2} + I_{S_1}^{DL} + N_0}, \tag{5}$$

during non ABS transmission, while SINR expression during ABS transmission is given by

$$SINR_{u_2}^{DL\_ABS} = \frac{P_{S_2} |h_{S_2^*,u_2^0}|^2 R_{S_2^*,u_2^0}{}^{-\alpha_2}}{I_{u_2}^{UL} + I_{S_2} + N_0}, \tag{6}$$

where

$$I_{u_2}^{UL} = \sum_{u_2 \in \Phi_{U_2}} P_{u_2} |h_{u_2,u_2^0}|^2 R_{u_2,u_2^0}{}^{-\alpha_2},$$
$$I_{S_2} = \sum_{S_2 \in \Phi_{S_2} \setminus S_2^*} P_{S_2} |h_{S_2,u_2^0}|^2 R_{S_2,u_2^0}{}^{-\alpha_2},$$
$$I_{S_1}^{DL} = \sum_{S_1 \in \Phi_{S_1}} P_{S_1} |h_{S_1,u_2^0}|^2 R_{S_1,u_2^0}{}^{-\alpha_1}.$$

given $I_{u_2}^{UL}$ is the interference from small cell uplink users, I_{S_2} is the interference from small cell BSs and $I_{S_1}^{DL}$ is the interference from other macrocell BSs.

In (5) and (6), $h_{S_2^*,u_2^0}$, h_{u_2,u_2^0}, h_{S_2,u_2^0}, and h_{S_1,u_2^0} denote the small scale fading channel coefficient for the channels of the downlink typical small cell user and its serving small cell BS, small cell users, small cell BSs and macrocell BSs, respectively. Further, $R_{S_2^*,u_2^0}$, R_{u_2,u_1^0}, R_{S_2,u_1^0}, and R_{S_1,u_1^0} denote the distances between the typical small cell downlink user and its associated small cell BS, small cell users, other interfering small cell BSs, and macrocell BSs, respectively.

C. UPLINK SINR OF SMALL CELL BS

We assume that UL users utilize distance-proportional fractional power control of the form $R_x^{\alpha\epsilon}$ [23], where $\epsilon \in [0, 1]$ is the power control factor. Therefore, as users moves closer to the associated BS, the transmit power required to maintain the same received signal power decreases, which is a key issue for battery-limited users.

For a typical small cell BS in the uplink located at the origin S_2^0, the SINR can be expressed as

$$SINR_{S_2}^{UL} = \frac{P_{u_2} |h_{u_2^*,S_2^0}|^2 R_{u_2^*,S_2^0}{}^{\alpha_2(\epsilon-1)}}{RSI + I_{u_2}^{UL} + I_{S_2} + I_{S_1}^{DL} + N_0}, \tag{7}$$

during non ABS transmission, while SINR expression during ABS transmission is given by

$$SINR_{S_2}^{UL\_ABS} = \frac{P_{u_2} |h_{u_2^*,S_2^0}|^2 R_{u_2^*,S_2^0}{}^{\alpha_2(\epsilon-1)}}{RSI + I_{u_2}^{UL} + I_{S_2} + N_0}, \tag{8}$$

where

$$I_{u_2}^{UL} = \sum_{u_2 \in \Phi_{U_2}} P_{u_2} |h_{u_2,S_2^0}|^2 R_{u_2,S_2^0}{}^{\alpha_2\epsilon},$$
$$I_{S_2} = \sum_{S_2 \in \Phi_{S_2} \setminus S_2^*} P_{S_2} |h_{S_2,S_2^0}|^2 R_{S_2,S_2^0}{}^{\alpha_2\epsilon},$$
$$I_{S_1}^{DL} = \sum_{S_1 \in \Phi_{S_1}} P_{S_1} |h_{S_1,S_2^0}|^2 R_{S_1,S_2^0}{}^{\alpha_1\epsilon}.$$

given $I_{u_2}^{UL}$ denotes the interference from other small cell uplink users, I_{S_2} is the interference from other small cell BSs and $I_{S_1}^{DL}$ is the interference from macrocell BSs.

When $\epsilon = 1$, the numerator of (7) becomes $P_{u_2} |h_{u_2^*,S_2^0}|^2$, with the pathloss completely inverted by the power control, and when $\epsilon = 0$, no channel inversion is performed and all the nodes transmit using the same power.

In (7), $h_{u_2^*,S_2^0}$, h_{u_2,S_2^0}, h_{S_2,S_2^0}, and h_{S_1,S_2^0} denote the small scale fading channel coefficient for the channels of small cell uplink BS and its associated small cell uplink user, other interfering small cell uplink users, other small cell BSs and macrocell BSs, respectively. Moreover, $R_{u_2^*,S_2^0}$, R_{u_2,S_2^0}, R_{S_2,S_2^0}, and R_{S_1,S_2^0} denote the distances between the typical small cell uplink BS and its associated small cell uplink user, other interfering small cell uplink users, other small cell BSs and macrocell BSs, respectively.

III. OUTAGE PROBABILITY ANALYSIS

In this section, we analyze the outage probability of two-tier HCNs with FD small cells, which is a metric that represents the average fraction of the cell area that is in outage at any time. We define the outage probability as the probability that the instantaneous SINR of a randomly located user is less than a target SINR τ. Since the typical user is associated with at most one tier, from the law of total probability, the outage

probability is given as

$$\mathbb{O} = \sum_{k=1}^{K} \mathbb{O}_k \mathcal{A}_k, \tag{9}$$

where $\mathcal{A}_k$ is the per-tier association probability given in (3) and (2), and $\mathbb{O}_k$ is the outage probability of a typical user associated with k_{th} tier, and K denotes the number of tiers. For a target SINR τ_k and a typical user $\text{SINR}_k(x)$ at a distance x from its associated BS, the outage probability is given by

$$\mathbb{O}_k = \mathbb{E}\left[\mathbb{P}\left[SINR_k(x) < \tau_k\right]\right]. \tag{10}$$

Considering the chosen network model of HD macrocells and FD small cells, the expression of the outage probability becomes

$$\mathbb{O} = \mathbb{O}_1^{DL}\mathcal{A}_1 + (\mathbb{O}_2^{DL} + \mathbb{O}_2^{UL})\mathcal{A}_2, \tag{13}$$

where $\mathbb{O}_1^{DL}$, $\mathbb{O}_2^{DL}$ and $\mathbb{O}_2^{UL}$ denote the outage probability of macrocell downlink user, small cell downlink user, and small cell uplink BS, respectively, and are derived in the following section.

A. OUTAGE PROBABILITY OF MACROCELL DOWNLINK USER

The PDF of the distance between the typical macrocell user and the associated macrocell BS $R_{S_1^*,u_1^0}$, is given similar to [26] as

$$f_{R_{S_1^*,u_1^0}}(r) = \frac{2\pi\lambda_{S_1}}{\mathcal{A}_{S_1}} r \exp\left\{-\pi \sum_{j=1}^{2} \lambda_j \left(\frac{P_{S_j}}{P_{S_1}}\right)^{\frac{2}{\alpha_j/\alpha_1}}\right\}, \tag{14}$$

where $\mathcal{A}_{S_1}$ is given in (2).

Theorem 1: The outage probability $\mathbb{O}_1^{DL}$ in HCNs comprised of HD macrocell and FD small cell, is defined as the probability that the instantaneous SINR of a randomly located macrocell downlink user is lower than a target τ_1, and expressed as

$$\mathbb{O}_1^{DL} = 1 - \left\{\frac{2\pi\lambda_{S_1}}{\mathcal{A}_{S_1}} \int_0^{\infty} r \exp\left\{ - r^{\alpha_1} {P_{S_1}}^{-1} N_0 \tau_1 - \pi\left(\left(\Psi_1 r^{\frac{2}{\alpha_2/\alpha_1}}\right) + \left(\Psi_2 r^{\frac{2}{\alpha_2/\alpha_1}}\right) + \left(\Psi_3 r^2\right)\right)\right\} dr\right\}, \tag{15}$$

where

$$\Psi_1 = \lambda_{u_2}\left(\frac{P_{u_2}}{P_{S_1}}\right)^{2/\alpha_2} \frac{2\tau_1}{\alpha_2 - 2} {}_2F_1[1, 1 - \frac{2}{\alpha_2}; 2 - \frac{2}{\alpha_2}; -\tau_1],$$
$$\Psi_2 = \lambda_{S_2}\left(\frac{P_{S_2}}{P_{S_1}}\right)^{2/\alpha_2} \frac{2\tau_1}{\alpha_2 - 2} {}_2F_1[1, 1 - \frac{2}{\alpha_2}; 2 - \frac{2}{\alpha_2}; -\tau_1],$$
$$\Psi_3 = \lambda_{S_1}\left(\frac{P_{S_1}}{P_{S_1^*}}\right)^{2/\alpha_1} \frac{2\tau_1}{\alpha_1 - 2} {}_2F_1[1, 1 - \frac{2}{\alpha_1}; 2 - \frac{2}{\alpha_1}; -\tau_1],$$

with ${}_2F_1[\cdot]$ denote the Gauss hypergeometric function, and the pathloss exponents $\alpha_j > 2$.

Proof: See Appendix A. □

B. OUTAGE PROBABILITY OF SMALL CELL DOWNLINK USER

The PDF of the distance between the typical small cell downlink user and its associated BS $R_{S_2^*,u_2^0}$, is given similar to [26] as

$$f_{R_{S_2^*,u_2^0}}(r) = \frac{2\pi\lambda_{S_2}}{\mathcal{A}_{S_2}} r \exp\left\{-\pi \sum_{j=1}^{2} \lambda_j (P_{S_j}/P_{S_2})^{\frac{2}{\alpha_j/\alpha_2}}\right\}. \tag{16}$$

Theorem 2: The outage probability $\mathbb{O}_2^{DL}$ in HCNs comprised of HD macrocell and FD small cell, is defined as the probability that the instantaneous SINR of a randomly located small cell downlink user is lower than a target τ_2, during transmission of both ABS and non-ABS subframes, and expressed as (11) *at the bottom of this page, where*

$$\eta_1 = \lambda_{u_2}\left(\frac{P_{u_2}}{P_{S_2}}\right)^{2/\alpha_2} \frac{2\tau_2}{\alpha_2 - 2} {}_2F_1[1, 1 - \frac{2}{\alpha_2}; 2 - \frac{2}{\alpha_2}; -\tau_2],$$
$$\eta_2 = \lambda_{S_2}\left(\frac{P_{S_2}}{P_{S_2^*}}\right)^{2/\alpha_2} \frac{2\tau_2}{\alpha_2 - 2} {}_2F_1[1, 1 - \frac{2}{\alpha_2}; 2 - \frac{2}{\alpha_2}; -\tau_2],$$
$$\eta_3 = \lambda_{S_1}\left(\frac{P_{S_1}}{P_{S_2}}\right)^{2/\alpha_1} \frac{2\tau_2}{\alpha_1 - 2} {}_2F_1[1, 1 - \frac{2}{\alpha_1}; 2 - \frac{2}{\alpha_1}; -\tau_2],$$

for the pathloss exponents $\alpha_j > 2$.

Proof: See Appendix B □

C. OUTAGE PROBABILITY OF SMALL CELL UPLINK BS

Since macrocells can only service one DL active user at a time, the UL users can only be associated to the FD small cells. Therefore, we assume that UL users are associated with

$$\mathbb{O}_2^{DL} = 1 - \left\{\frac{2\pi(1-\rho)\lambda_{S_2}}{\mathcal{A}_{S_2}} \int_0^{\infty} r \exp\left\{ - r^{\alpha_2} {P_{S_2}}^{-1} N_0 \tau_2 - \pi\left(\left(\eta_1 r^2\right) + \left(\eta_2 r^{\frac{2}{\alpha_2/\alpha_1}}\right) + \left(\eta_3 r^{\frac{2}{\alpha_1/\alpha_2}}\right)\right)\right\} dr + \frac{2\pi\rho\lambda_{S_2}}{\mathcal{A}_{S_2}} \int_0^{\infty} r \exp\left\{ - r^{\alpha_2} {P_{S_2}}^{-1} N_0 \tau_2 - \pi\left(\left(\eta_1 r^2\right) + \left(\eta_2 r^{\frac{2}{\alpha_2/\alpha_1}}\right)\right)\right\} dr\right\}, \tag{11}$$

$$\mathbb{O}_2^{UL} = 1 - \left\{2\pi(1-\rho)\lambda_{S_2} \int_0^{\infty} r \exp\left\{ - r^{\alpha_2(\epsilon-1)} {P_{u_2}}^{-1} P_{S_2} \sigma_e^2 N_0 \tau_3 - \pi\left(\left(\Gamma_1 r^2\right) + \left(\Gamma_2 r^2\right) + \left(\Gamma_3 r^{\frac{2}{\alpha_1/\alpha_2}}\right)\right)\right\} dr + 2\pi\rho\lambda_{S_2} \int_0^{\infty} r \exp\left\{ - r^{\alpha_2(\epsilon-1)} {P_{u_2}}^{-1} P_{S_2} \sigma_e^2 N_0 \tau_3 - \pi\left(\left(\Gamma_1 r^2\right) + \left(\Gamma_2 r^2\right)\right)\right\} dr\right\}, \tag{12}$$

the small cells based on the nearest BS association rule, where the PDF of the distance between the UL users and the small cells $R_{S_2,u_2^{UL}}$, is given similar to [26] as

$$f_{R_{S_2,u_2^{UL}}}(r) = e^{-\lambda_2 \pi r^2} 2\pi\lambda_2 r. \tag{17}$$

Theorem 3: The outage probability $\mathbb{O}_2^{UL}$ in HCNs comprised of HD macrocell and FD small cell, is defined as the probability that the instantaneous SINR of a randomly located UL small cell BS is lower than a target τ_3 during both ABS and non-ABS subframes is given by (12) *at the bottom of the previous page, where*

$$\Gamma_1 = \lambda_{u_2} \frac{2\tau_3}{\alpha_2 - 2} {}_2F_1[1, 1 - \frac{2}{\alpha_2\epsilon}; 2 - \frac{2}{\alpha_2\epsilon} - \tau_3]$$

$$\Gamma_2 = \lambda_{S_2} \left(\frac{P_{S_2}}{P_{u_2}}\right)^{2/\alpha_2\epsilon} \frac{2\tau_3}{\alpha_2 - 2} {}_2F_1[1, 1 - \frac{2}{\alpha_2\epsilon}; 2 - \frac{2}{\alpha_2\epsilon} - \tau_3]$$

$$\Gamma_3 = \lambda_{S_1} \left(\frac{P_{S_1}}{P_{u_2}}\right)^{2/\alpha_1\epsilon} \frac{2\tau_3}{\alpha_1 - 2} {}_2F_1[1, 1 - \frac{2}{\alpha_1\epsilon}; 2 - \frac{2}{\alpha_1\epsilon}; -\tau_3],$$

for $\alpha_j > 2$.

Proof: See Appendix C. □

IV. RATE COVERAGE ANALYSIS

In this section, we analyze the rate coverage of two-tier HCNs with FD small cells. The rate coverage is defined in [33] as the probability that a randomly chosen user can achieve a target rate ϖ, which is given by

$$\Theta \triangleq \mathbb{P}(\mathcal{R} > \varpi). \tag{19}$$

Since the DL users can associate with either macro cells or small cells in *open-access* mode, the overall rate coverage for the chosen user in two-tier HCNs is given by

$$\Theta = \mathcal{A}_{S_1}\mathbb{P}\left(\mathcal{R}_{S_1} > \varpi | \mathcal{A}_{S_1}\right) + \mathcal{A}_{S_2}\mathbb{P}\left(\mathcal{R}_{S_2} > \varpi | \mathcal{A}_{S_2}\right), \tag{20}$$

where $\mathcal{A}_{S_1}$ and $\mathcal{A}_{S_2}$ denote the probability that a user is associated with the macrocell or the small cell, and $\mathbb{P}\left(\mathcal{R}_{S_1} > \varpi | \mathcal{A}_{S_1}\right)$ and $\mathbb{P}\left(\mathcal{R}_{S_2} > \varpi | \mathcal{A}_{S_2}\right)$ denote the rate coverage conditioned on the association with the former and the latter, respectively.

The rate achieved by a user associated with the tagged BS in the x^{th}-tier is given by

$$\mathcal{R}_x = \frac{W}{\mathcal{N}_x} \log_2(1 + SINR_x), \tag{21}$$

where W is the bandwidth of the frequency band, $\mathcal{N}_x$ is a random variable which denotes the average number of users associated with the tagged base station in the x^{th}-tier, and $SINR_x$ is the received signal-to-interference-plus-noise-ratio from the serving base station for a user.

A. RATE COVERAGE FOR MACROCELL USERS IN THE DOWNLINK

In Rayleigh fading environments, the rate coverage for a macrocell DL user is given by

$$\begin{aligned}
&\mathbb{P}\left(\mathcal{R}_{S_1} > \varpi | \mathcal{A}_{S_1}\right) \\
&= \mathbb{E}_{\mathcal{N}_{S_1}}\left[\mathbb{P}\left(SINR_{u_1}^{DL} > 2^{\frac{\varpi \mathcal{N}_{S_1}}{W}} - 1 | \mathcal{A}_{S_1}\right)\right] \\
&= \sum_{n\geq 0} \mathbb{P}\left(\frac{P_{S_1} h_{S_1^*,u_1^0} R_{S_1^*,u_1^0}^{-\alpha_1}}{I} > \kappa_1 | \mathcal{A}_{S_1}\right) \\
&\quad \times \mathbb{P}\left(\mathcal{N}_{S_1} = n + 1\right),
\end{aligned} \tag{22}$$

where $I = I_{u_2}^{UL} + I_{S_2} + I_{S_1}^{DL} + N_0$ is the cumulative interference from small cell UL users along with macrocell and small cell BSs, and the additive Gaussian noise, and $\kappa_1 = 2^{\frac{\varpi \mathcal{N}_{S_1}}{W}} - 1$.

According to [33], the distribution of the load associated with the x^{th}-tier is given by

$$\begin{aligned}
&\mathbb{P}\left(\mathcal{N}_x = n + 1\right) \\
&= \frac{3.5^{3.5}}{n!} \frac{\Gamma(n + 4.5)}{\Gamma(3.5)} \left(\frac{\lambda_u \mathcal{A}_x}{\lambda_x}\right)^n \left(3.5 + \frac{\lambda_u \mathcal{A}_x}{\lambda_x}\right)^{-n-4.5},
\end{aligned} \tag{23}$$

with the mean load $\mathbb{E}[\mathcal{N}_x] = 1 + 1.28\frac{\lambda_u \mathcal{A}_x}{\lambda_x}$, where $\Gamma(x) = \int_0^\infty t^{x-1} e^{-t} dt$ is the Gamma function, and $\mathcal{A}_x$ denotes the association probability of the x^{th}-tier. Hence,

$$\begin{aligned}
&\mathbb{P}\left(\frac{P_{S_1} h_{S_1^*,u_1^0} R_{S_1^*,u_1^0}^{-\alpha_1}}{I} > \kappa_1 | \mathcal{A}_{S_1}\right) \\
&= \int_0^\infty \mathbb{P}\left(\frac{P_{S_1} h_{S_1^*,u_1^0} R_{S_1^*,u_1^0}^{-\alpha_1}}{I} > \kappa_1\right) f_{R_{S_1^*,u_1^0}}(r) \\
&= \frac{2\pi\lambda_{S_1}}{\mathcal{A}_{S_1}} \int_0^\infty \mathbb{P}\left(\frac{P_{S_1} h_{S_1^*,u_1^0} R_{S_1^*,u_1^0}^{-\alpha_1}}{I} > \kappa_1\right) r \\
&\quad \times \exp\left\{-\pi \sum_{j=1}^{2} \lambda_j \left(\frac{P_j}{P_{S_1}}\right)^{\frac{2}{\alpha_j/\alpha_1}} r^{\frac{2}{\alpha_j/\alpha_1}}\right\} dr.
\end{aligned} \tag{24}$$

Using the derivation of outage probability for macrocell DL users and (23), the final expression for DL rate coverage of macrocell users can be obtained through (22).

$$\begin{aligned}
&\frac{2\pi(1-\rho)\lambda_{S_2}}{\mathcal{A}_{S_2}} \int_0^\infty \mathbb{P}\left(\frac{P_{S_2} h_{S_2^*,u_2^0} R_{S_2^*,u_2^0}^{-\alpha_2}}{I} > \kappa_2\right) r \exp\left\{-\pi \sum_{j=1}^{2} \lambda_j \left(\frac{P_j}{P_{S_2}}\right)^{\frac{2}{\alpha_j/\alpha_2}} r^{\frac{2}{\alpha_j/\alpha_2}}\right\} dr \\
&+ \frac{2\pi\rho\lambda_{S_2}}{\mathcal{A}_{S_2}} \int_0^\infty \mathbb{P}\left(\frac{P_{S_2} h_{S_2^*,u_2^0} R_{S_2^*,u_2^0}^{-\alpha_2}}{I'} > \kappa_2\right) r \exp\left\{-\pi \sum_{j=1}^{2} \lambda_j \left(\frac{P_j}{P_{S_2}}\right)^{\frac{2}{\alpha_j/\alpha_2}} r^{\frac{2}{\alpha_j/\alpha_2}}\right\} dr.
\end{aligned} \tag{18}$$

$$2\pi\ (1-\rho)\lambda_{S_2}\int_0^{\infty}\mathbb{P}\left(\frac{P_{S_2}h_{u_2^0,S_2^*}R_{u_2^0,S_2^*}{}^{-\alpha_2(\epsilon-1)}}{I+RSI}>\kappa_2\right)r\exp\left\{-\pi\sum_{j=1}^{2}\lambda_j\left(\frac{P_j}{P_{S_2}}\right)^{\frac{2}{\alpha_j/\alpha_2}}r^{\frac{2}{\alpha_j/\alpha_2}}\right\}dr$$
$$+2\pi\rho\lambda_{S_2}\int_0^{\infty}\mathbb{P}\left(\frac{P_{S_2}h_{u_2^0,S_2^*}R_{u_2^0,S_2^*}{}^{-\alpha_2(\epsilon-1)}}{I'+RSI}>\kappa_2\right)r\exp\left\{-\pi\sum_{j=1}^{2}\lambda_j\left(\frac{P_j}{P_{S_2}}\right)^{\frac{2}{\alpha_j/\alpha_2}}r^{\frac{2}{\alpha_j/\alpha_2}}\right\}dr. \quad (25)$$

B. RATE COVERAGE FOR SMALL CELL USERS IN THE DOWNLINK

Following the same derivation approach, the rate coverage for DL small cell users is given by

$$\begin{aligned}&\mathbb{P}\left(\mathcal{R}_{S_2}^{DL}>\varpi|\mathcal{A}_{S_2}\right)\\&=\mathbb{E}_{\mathcal{N}_{S_2}}\Big[\rho\mathbb{P}\left(SINR_{u_2}^{DL\_ABS}>2^{\frac{\varpi\mathcal{N}_{S_2}}{W}}-1|\mathcal{A}_{S_2}\right)\\&\quad+(1-\rho)\mathbb{P}\left(SINR_{u_2}^{DL}>2^{\frac{\varpi\mathcal{N}_{S_2}}{W}}-1|\mathcal{A}_{S_2}\right)\Big]\\&=\Bigg[(1-\rho)\sum_{n\geq0}\mathbb{P}\left(\frac{P_{S_2}h_{S_2^*,u_2^0}R_{S_2^*,u_2^0}{}^{-\alpha_2}}{I}>\kappa_2|\mathcal{A}_{S_2}\right)\\&\quad+\rho\sum_{n\geq0}\mathbb{P}\left(\frac{P_{S_2}h_{S_2^*,u_2^0}R_{S_2^*,u_2^0}{}^{-\alpha_2}}{I'}>\kappa_2|\mathcal{A}_{S_2}\right)\Bigg]\\&\quad\times\mathbb{P}\left(\mathcal{N}_{S_2}=n+1\right),\end{aligned} \quad (26)$$

where $I=I_{u_2}^{UL}+I_{S_2}+I_{S_1}^{DL}+N_0$ denote the cumulative interference from small cell UL users along with macrocell and small cell BSs, receptively. $I'=I_{u_2}^{UL}+I_{S_2}+N_0$ is the cumulative interference during ABS transmission, and $\kappa_2=2^{\frac{\varpi\mathcal{N}_{S_2}}{W}}-1$.

Using the load distribution given in (23), (27) and (28), we obtain (18) at the bottom of the previous page

$$(1-\rho)\mathbb{P}\left(\frac{P_{S_2}h_{S_2^*,u_2^0}R_{S_2^*,u_2^0}{}^{-\alpha_2}}{I}>\kappa_2|\mathcal{A}_{S_2}\right)=(1-\rho)$$
$$\times\int_0^{\infty}\mathbb{P}\left(\frac{P_{S_2}h_{S_2^*,u_2^0}R_{S_2^*,u_2^0}{}^{-\alpha_2}}{I}>\kappa_2\right)f_{R_{S_2^*,u_2^0}}(r). \quad (27)$$

$$\rho\mathbb{P}\left(\frac{P_{S_2}h_{S_2^*,u_2^0}R_{S_2^*,u_2^0}{}^{-\alpha_2}}{I'}>\kappa_2|\mathcal{A}_{S_2}\right)$$
$$=\rho\int_0^{\infty}\mathbb{P}\left(\frac{P_{S_2}h_{S_2^*,u_2^0}R_{S_2^*,u_2^0}{}^{-\alpha_2}}{I'}>\kappa_2\right)f_{R_{S_2^*,u_2^0}}(r). \quad (28)$$

Finally, Using the derivation of outage probability for small cell DL users and (23), the final expression for rate coverage of small cell DL users can be obtained through (26).

C. RATE COVERAGE FOR SMALL CELL BS IN THE UPLINK

Similarly, the rate coverage for UL small cell BS is given by

$$\begin{aligned}&\mathbb{P}\left(\mathcal{R}_{S_2}^{UL}>\varpi|\mathcal{A}_{S_2}\right)\\&=\mathbb{E}_{\mathcal{N}_{S_2}}\Big[\rho\mathbb{P}\left(SINR_{u_2}^{UL\_ABS}>2^{\frac{\varpi\mathcal{N}_{S_2}}{W}}-1|\mathcal{A}_{S_2}\right)\\&\quad+(1-\rho)\mathbb{P}\left(SINR_{u_2}^{UL}>2^{\frac{\varpi\mathcal{N}_{S_2}}{W}}-1|\mathcal{A}_{S_2}\right)\Big].\\&=\Bigg[(1-\rho)\sum_{n\geq0}\mathbb{P}\left(\frac{P_{S_2}h_{u_2^0,S_2^*}R_{u_2^0,S_2^*}{}^{-\alpha_2(\epsilon-1)}}{I+RSI}>\kappa_2|\mathcal{A}_{S_2}\right)\\&\quad+\rho\sum_{n\geq0}\mathbb{P}\left(\frac{P_{S_2}h_{u_2^0,S_2^*}R_{u_2^0,S_2^*}{}^{-\alpha_2(\epsilon-1)}}{I'+RSI}>\kappa_2|\mathcal{A}_{S_2}\right)\Bigg]\\&\quad\times\mathbb{P}\left(\mathcal{N}_{S_2}=n+1\right),\end{aligned} \quad (29)$$

where $I=I_{u_2}^{UL}+I_{S_2}+I_{S_1}^{DL}+N_0$ is the cumulative interference from UL small cell users along with macrocell and small cell BSs, and the Gaussian additive noise. $I'=I_{u_2}^{UL}+I_{S_2}+N_0$ is the cumulative interference during ABS transmission.

Using the load distribution given in (23) and both (30) and (31) we obtain (25) at the top of this page

$$(1-\rho)\mathbb{P}\left(\frac{P_{S_2}h_{u_2^0,S_2^*}R_{u_2^0,S_2^*}{}^{-\alpha_2(\epsilon-1)}}{I+RSI}>\kappa_2|\mathcal{A}_{S_2}\right)$$
$$=(1-\rho)\int_0^{\infty}\mathbb{P}\left(\frac{P_{S_2}h_{u_2^0,S_2^*}R_{u_2^0,S_2^*}{}^{-\alpha_2(\epsilon-1)}}{I+RSI}>\kappa_2\right)$$
$$\times f_{R_{S_2,u_2^{UL}}}(r). \quad (30)$$

$$\rho\mathbb{P}\left(\frac{P_{S_2}h_{u_2^0,S_2^*}R_{u_2^0,S_2^*}{}^{-\alpha_2(\epsilon-1)}}{I+RSI}>\kappa_2|\mathcal{A}_{S_2}\right)$$
$$=\rho\int_0^{\infty}\mathbb{P}\left(\frac{P_{S_2}h_{u_2^0,S_2^*}R_{u_2^0,S_2^*}{}^{-\alpha_2(\epsilon-1)}}{I+RSI}>\kappa_2\right)f_{R_{S_2,u_2^{UL}}}(r). \quad (31)$$

Finally, Using the derivation of outage probability for UL small cell BS and (23), the final expression for rate coverage of UL small cell BS can be obtained through (29).

V. NUMERICAL AND SIMULATION RESULTS

In this section, we evaluate the performance of two-tier HCNs with FD small cells. Specifically, we investigate how different parameters affect network performance in terms of the outage probability and the rate coverage. The simulation methodology comprises independent realization of PPP distributions

TABLE 2. Parametric values (unless otherwise specified).

Parameter	Value
$\lambda_x \ \forall x$	$(\pi \times 500^2)^{-1}$
P_{S_1} [dBm]	43 dBm (20 W)
$P_{S,2}$ [dBm]	23 dBm (200 mW)
$P_{u_y} \ \forall y$ [dBm]	23 dBm (200 mW)
W [Hz]	10^7
$\alpha_k \ \forall k$	4
$\tau_n \ \forall n$ [dB]	0 dB
RSI	$P_{S_2} 10^{L_{dB}/10}$
L_{dB} [dB]	-38 dB
ρ	0.3
ϵ	0.2

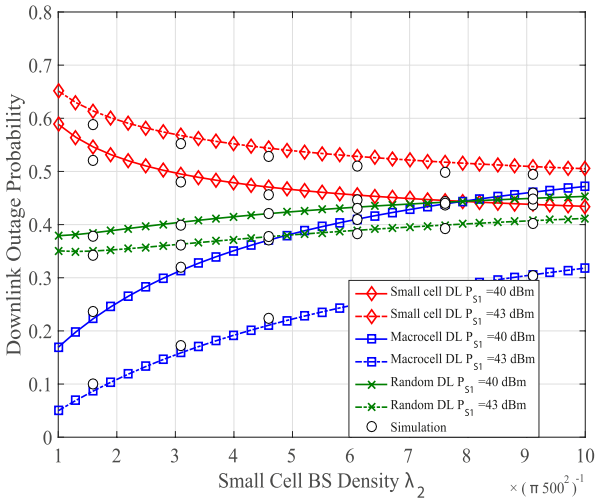

FIGURE 2. Outage probability of macrocell and small cell downlink as a function of small cell density λ_2.

for the BSs of two tiers, followed by realization of user distribution and the association process. After that, outage probability and rate coverage are calculated based on the cumulative interference. The parameters used for the analysis and simulation are stated in Table 2. Monte Carlo simulations have been conducted to obtain the results, averaged over 10000 iterations, which are then compared with numerical evaluation of the derived expressions.

Fig. 2 plots the outage probability of a typical DL user associated with macrocell BS, small cell BS, and random type of BS in the DL, as a function of small cell BSs density λ_2. We observe that the outage probability of macrocell DL user increases with increasing the small cell BS density. This results from the increase in aggregate interference from the small cell BSs, as shown in (4). Additionally, the outage probability of macrocell DL user decreases with increasing the transmit power at the macrocell BS, which is due to the increase in SINR at the typical downlink user associated with macrocell BS, as shown in (4). Interestingly, for the typical downlink user associated with small cell BS, the outage probability decreases with increasing the small cell BS density. This is because densification of tier 2 reduces the inter-link distances between the typical downlink user and

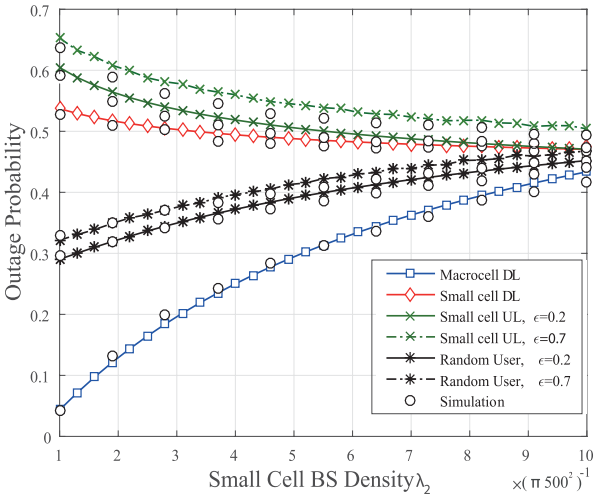

FIGURE 3. Outage probability as a function of small cell density λ_2.

the associated small cell BS, as shown in (5). In addition, the outage probability of typical small cell DL user increase with increasing the transmit power at the macrocell BS, which is due to the increase in aggregate interference caused by macrocell BSs, as shown in (5). Finally, outage probability of a random DL user, which is defined as $\mathbb{O}_1^{DL}\mathcal{A}_1 + \mathbb{O}_2^{DL}\mathcal{A}_2$, increases with both the increase of small cell density, and the decrease of transmit power of macrocell BS. This is because $\mathbb{O}_1^{DL}$ in the expression is lower than $\mathbb{O}_2^{DL}$, therefore the expression reflects such tendency. Note that the simulation results closely follow the analytical results, and therefore, validate the analytical modeling.

Fig. 3 plots the outage probability of macrocell DL user, small cell DL user, small cell UL BS, and a randomly located user versus the density of small cell BSs. In this figure, we focus on the impact of small cell BSs density on the outage probability of a randomly located user. Interestingly, we observe that the outage probability of a randomly located user is not significantly affected by the increase in the small cell BS density. It suffers from slight increase that results from aggregate interference from the small cell BSs, as shown in (13). We also evaluate the impact of uplink power control factor, ϵ on outage. As shown by the results, a higher value of ϵ results in a higher outage probability, for small cell user in the uplink, due to reduced uplink transmit power as a consequence of more aggressive power control. The simulation results also closely follow the analytical results.

Fig. 4 plots rate coverage for a random DL user and UL small cell BS versus the small cell BSs density. We note that the rate coverage of a random DL user decrease as the density of small cell BSs increases. This is because of increase in aggregate interference caused by small cell BSs, as seen in (4). Similarly, the rate coverage of a random DL user decreases with increasing the transmission power of small cell BSs. On the contrary, rate coverage of an UL small cell BS increase with increase of small cell BSs density. This is due to the fact that densification reduces the inter-link

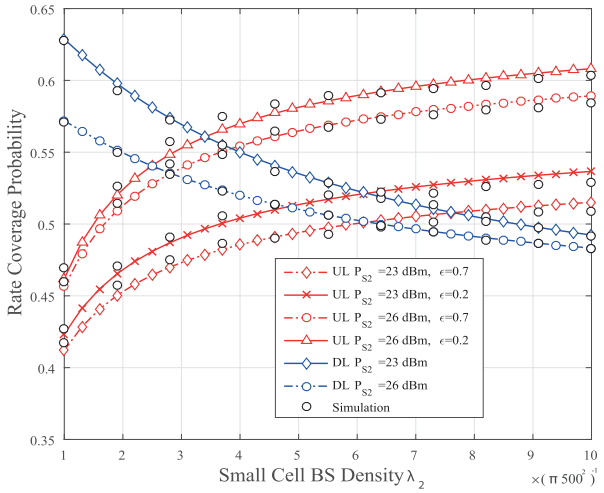

FIGURE 4. Rate coverage as a function of small cell density λ_2.

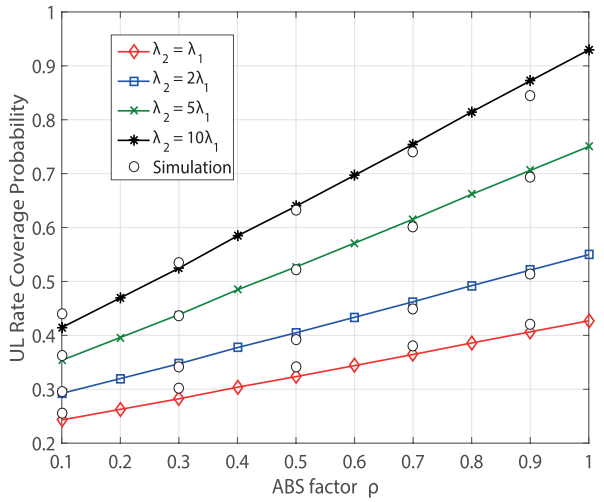

FIGURE 5. UL rate coverage probability as a function of ABS factor ρ.

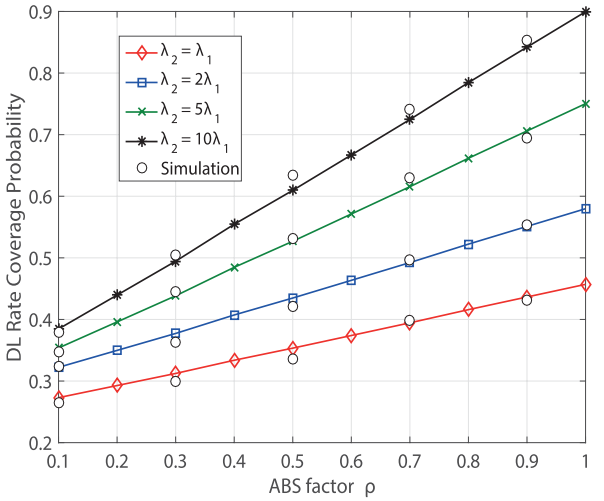

FIGURE 6. DL rate coverage probability as a function of ABS factor ρ.

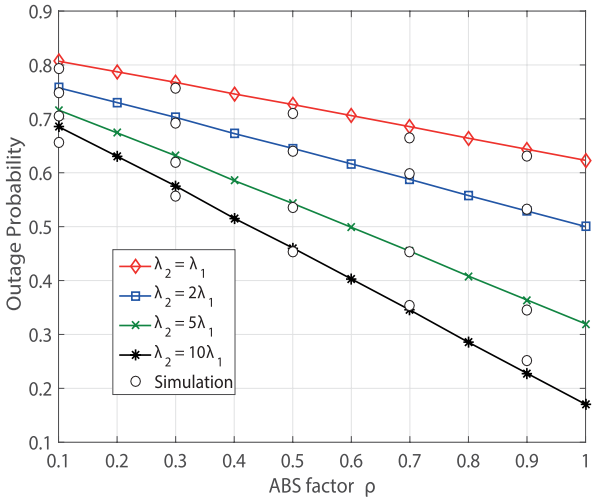

FIGURE 7. Outage probability in relation to ABS transmission factor ρ.

distance between a user and it's associated BS, which can be verified by (7). Similarly, the rate coverage of an UL small cell BS increases with increasing the transmission power of small cell BSs due to higher SINR of small cell UL BS as can be verified by (7). We also evaluate the impact of uplink power control factor, ϵ on rate coverage. As shown by the results, a higher value of ϵ results in a lower rate coverage probability, for small cell user in the uplink, due to reduced uplink transmit power as a consequence of more aggressive power control.

Fig. 5 plots the rate coverage of UL small cell BSs as a function of the ABS factor ρ. We note that the rate coverage of UL small cell BSs increases as ρ increases. This is because of the aggregate interference caused by macrocell BSs, which can be seen in (7) and (8). Similarly, in Fig. 6, the rate coverage of random DL users increases with increasing ρ for the same reason, which can be seen in (5) and (6). Fig. 7 shows that the outage probability of a random user decreases as ρ increases. This is due to the fact that interference originated by macrocell BSs decreases with increasing ρ, as seen in (4) and (6).

Fig. 8 plots the relation between small cell UL rate coverage probability and the residual SI cancellation $RSI = P_{S_2}.10^{L_{dB}/10}$, where L_{dB} is the ratio of RSI after interference cancellation is applied to the transmission power at the receiver. We observe that outage probability of a randomly located user is initially high, especially when SI cancellation capability is low ($L_{dB} < -15$), then it decreases with increasing L_{dB}, until it nearly stabilise beyond ($L_{dB} > -37$). This is because the high SI cancellation capabilities improve the performance of FD links as can be seen in (7). Additionally, we observe that the outage probability in high small cell densities is more sensitive to L_{dB} variations. This is due to increased FD links in higher small cell densities since only the small cell BSs operate in FD mode.

In Fig. 9, we plot the relation between small cell UL rate coverage probability and SI cancellation capability L_{dB}. Since

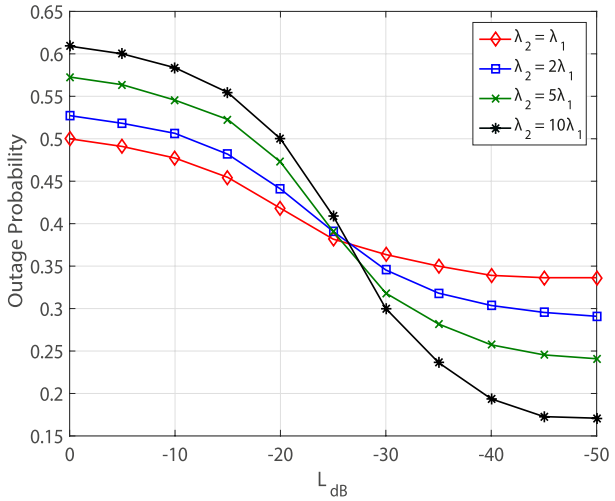

FIGURE 8. Outage probability as a function of the SI cancellation capability L_{dB}.

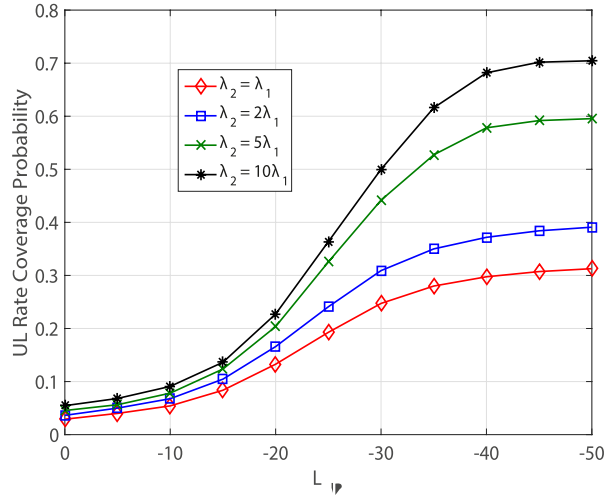

FIGURE 9. UL rate coverage probability as a function of the self-interference cancellation capability L_{dB}.

only the small cell BSs operate in FD mode, SI only applies to those BSs. We note that the rate coverage increases with the increase of L_{dB}. This is because higher SI cancellation improves the performance of FD links, as can be seen in (7) and (8). Moreover, increasing the density of small cell BSs increases the rate coverage. This is due to the fact that more FD links exist in higher small cell densities.

VI. CONCLUSIONS

Unprecedented technological developments like network densification and FD communications will be crucial in shaping 5G radio access networks for achieving the envisioned capacity objectives. Realizing the FD capability at small cells is particularly attractive due to simplicity, superior SI cancellation (compared to macrocells), and widespread deployment. In this paper, we have investigated the performance of two-tier interference-coordinated HCNs with FD small cells. We have derived closed-form expressions for outage probability and rate coverage in two-tier HCNs with FD small cells explicitly accounting for interference coordination between macro and small cells. Performance evaluation investigates the impact of different network parameters on both outage and rate coverage probabilities. The results demonstrate that the outage probability and the rate coverage improves with higher ABS factor and better underlying SI cancellation capabilities of FD small cells.

APPENDIX

A. PROOF OF THEOREM 1

From (10), the outage probability $\mathbb{O}_1^{DL}$ is given as

$$\begin{aligned}\mathbb{O}_1^{DL} &= \mathbb{E}\left[\mathbb{P}\left[SINR_{u_1}^{DL} < \tau_1\right]\right] \\ &= 1 - \int_0^\infty \mathbb{P}\left[SINR_{u_1}^{DL} > \tau_1\right] f_{R_{S_1^*,u_1^0}}(r)dr \\ &= 1 - \frac{2\pi\lambda_{S_1}}{\mathcal{A}_{S_1}} \int_0^\infty \mathbb{P}\left[SINR_{u_1}^{DL} > \tau_1\right] r \\ &\quad \times \exp\left\{-\pi \sum_{j=1}^{2} \lambda_j \left(\frac{P_{S_j}}{P_{S_1}}\right)^{\zeta_1} r^{\zeta_1}\right\} dr, \end{aligned} \tag{32}$$

where $\zeta_1 = \frac{2}{\alpha_j/\alpha_1}$.

By setting $Q_1 = I_{u_2}^{UL} + I_{S_2} + I_{S_1}^{DL} + N_0$, We rewrite $SINR_{u_1}^{DL}$ as $\frac{h_{S_1^*,u_1}}{{P_{S_1}}^{-1} r^{\alpha_1} Q_1}$. Therefore,

$$\begin{aligned}&\mathbb{P}\left[SINR_{u_1}^{DL} > \tau_1\right] \\ &= \mathbb{P}\left[h_{S_1,u_1} > {P_{S_1}}^{-1} r^{\alpha_1} \tau_1 \, Q_1\right] \\ &= \int_0^\infty \exp\{-r_{S_1^*,u_1^0}^{\alpha_{S_1^*,u_1^0}} {P_{S_1}}^{-1} \tau_1 \, q_1\} f_{Q_1}(q_1) dq_1 \\ &= \mathbb{E}_{Q_1}\left[\exp\{-r^{\alpha_1} {P_{S_1}}^{-1} \tau_1 \, q_1\}\right] \\ &= \exp\left\{-r^{\alpha_1} {P_{S_1}}^{-1} N_0 \tau_1\right\} \mathcal{L}_{I_{u_2}^{UL}}(r^{\alpha_1} {P_{S_1}}^{-1} \tau_1) \\ &\quad \times \mathcal{L}_{I_{S_2}}(r^{\alpha_1} {P_{S_1}}^{-1} \tau_1) \mathcal{L}_{I_{u_1}^{DL}}(r^{\alpha_1} {P_{S_1}}^{-1} \tau_1). \end{aligned} \tag{33}$$

Starting with the Laplace transform of the interference originated from small cell UL users on the macrocell DL user, presented in (33), we have

$$\begin{aligned}&\mathcal{L}_{I_{u_2}^{UL}}(r^{\alpha_1} {P_{S_1}}^{-1} \tau_1) \\ &= \mathbb{E}_{I_{u_2}^{UL}}\left[\exp\left\{-r^{\alpha_1} {P_{S_1}}^{-1} \tau_1 \, I_{u_2}^{UL}\right\}\right] \\ &= \mathbb{E}_{\Phi_{U_2}}\left[\exp\left\{-r^{\alpha_1} \frac{P_{u_2}}{P_{S_1}} \tau_1 \sum_{u_2 \in \Phi_{U_2}} \mathrm{h}_{u_2,u_1^0} R_{u_2,u_1^0}^{-\alpha_2}\right\}\right] \\ &\overset{(b)}{=} \exp\left\{-2\pi\lambda_{u_2} \int_0^\infty 1 - \mathcal{L}_{h_{S_1,u_1}}\left(r^{\alpha_1} \frac{P_{u_2}}{P_{S_1}} \tau_1 x^{-\alpha_2}\right) x dx\right\} \\ &= \exp\left\{-2\pi\lambda_{S_1} \int_0^\infty \left(1 - \frac{1}{1 + r^{\alpha_1} \frac{P_{S_1}}{P_{S_1^*}} \tau_1 x^{-\alpha_1}}\right) x dx\right\} \\ &= \exp\left\{-2\pi\lambda_{u_2} \int_0^\infty \frac{x}{1 + \left(r^{\alpha_1} \frac{P_{u_2}}{P_{S_1}} \tau_1\right)^{-1} x^{\alpha_2}} dx\right\}. \end{aligned} \tag{34}$$

where (b) is provided in [41]. Note that the integration limits in (34) are from 0 to ∞ since the small cell UL users can be at any distance from the DL macrocell users. Now, with a change of variables $v_1 = (r^{\alpha_1}\frac{P_{u_2}}{P_{S_1}}\tau_1)^{-2/\alpha_2}x^2$, We express

$$\mathcal{L}_{I_{u_2}^{UL}}(r^{\alpha_1}{P_{S_1}}^{-1}\tau_1) = \exp\Big\{-\pi\lambda_{u_2}\Big(\frac{P_{u_2}}{P_{S_1}}\Big)^{2/\alpha_2} \times Z_1(\tau_1,\alpha_2)r^{\frac{2}{\alpha_2/\alpha_1}}\Big\}, \quad (35)$$

where

$$Z_1(\tau_1,\alpha_2) = \tau_1^{2/\alpha_2}\int_{x_1}^{\infty}\frac{1}{1+v_1^{\alpha_2/2}}dv_1 = \frac{2\tau_1}{\alpha_2-2}{}_2F_1[1,1-2/\alpha_2;2-2/\alpha_2;-\tau_1]. \quad (36)$$

In (36), ${}_2F_1[\cdot]$ denote the Gauss hypergeometric function and $x_1 = (1/\tau_1)^{2/\alpha_2}$. The expression holds for $\alpha_2 > 2$.

Similarly, we can derive the Laplace transform for the interference from small cells BSs expressed in (33), as

$$\mathcal{L}_{I_{S_2}}(r^{\alpha_1}{P_{S_1}}^{-1}\tau_1) = \exp\Big\{-\pi\lambda_{S_2}(P_{S_2}/P_{S_1})^{2/\alpha_2} \times\frac{2\tau_1}{\alpha_2-2}{}_2F_1[1,1-2/\alpha_2;2-2/\alpha_2;-\tau_1]\Big\}, \quad (37)$$

for $\alpha_2 > 2$. We finally derive the Laplace transform for the interference originated from macrocell BSs expressed in (33) using similar approach, as

$$\mathcal{L}_{I_{S_1}^{DL}}(r^{\alpha_1}{P_{S_1}}^{-1}\tau_1) = \exp\Big\{-\pi\lambda_{S_1}\Big(P_{S_1}/P_{S_1^*}\Big)^{2/\alpha_1} \times\frac{2\tau_1}{\alpha_1-2}{}_2F_1[1,1-2/\alpha_1,-\tau_1]\Big\}, \quad (38)$$

for $\alpha_1 > 2$. Now, plugging (35), (37) and (38) into $\mathbb{P}[SINR_{u_1}^{DL} > \tau_1]$ we obtain

$$\mathbb{P}[SINR_{u_1}^{DL} > \tau_1] = \exp\Big\{-r^{\alpha_1}{P_{S_1}}^{-1}N_0\tau_1 - \pi\Big(\Big(\Psi_1 r^{\frac{2}{\alpha_2/\alpha_1}}\Big)+\Big(\Psi_2 r^{\frac{2}{\alpha_2/\alpha_1}}\Big)+\Big(\Psi_3 r^2\Big)\Big)\Big\}. \quad (39)$$

given

$$\Psi_1 = \lambda_{u_2}\Big(\frac{P_{u_2}}{P_{S_1}}\Big)^{2/\alpha_2}\frac{2\tau_1}{\alpha_2-2}{}_2F_1[1,1-2/\alpha_2;2-2/\alpha_2;-\tau_1],$$

$$\Psi_2 = \lambda_{S_2}\Big(\frac{P_{S_2}}{P_{S_1}}\Big)^{2/\alpha_2}\frac{2\tau_1}{\alpha_2-2}{}_2F_1[1,1-2/\alpha_2;2-2/\alpha_2;-\tau_1],$$

$$\Psi_3 = \lambda_{S_1}\Big(\frac{P_{S_1}}{P_{S_1^*}}\Big)^{2/\alpha_1}\frac{2\tau_1}{\alpha_1-2}{}_2F_1[1,1-2/\alpha_1;2-2/\alpha_2;-\tau_1],$$

where $\alpha_j > 2$. Therefore, the final expression for a randomly located macrocell DL user is given by (15).

B. PROOF OF THEOREM 2

From (10), the outage probability $\mathbb{O}_2^{DL}$, considering the adapted eICIC mechanism is given by

$$\mathbb{O}_2^{DL} = (1-\rho)\mathbb{E}\Big[\mathbb{P}\Big[SINR_{u_2}^{DL} < \tau_2\Big]\Big] + \rho\mathbb{E}\Big[\mathbb{P}\Big[SINR_{u_2}^{DL\_ABS} < \tau_2\Big]\Big], \quad (40)$$

where ρ is the ABS transmission ratio.

Starting by the first term of (40), we have

$$\begin{aligned}(1-\rho)\mathbb{E}\Big[\mathbb{P}\Big[SINR_{u_2}^{DL} > \tau_2\Big]\Big] &= 1-\Big((1-\rho)\int_0^{\infty}\mathbb{P}\Big[SINR_{u_2}^{DL} > \tau_2\Big]f_{R_{S_2^*,u_2^0}}(r)dr\Big)\\ &= 1-\frac{2\pi\ (1-\rho)\lambda_{S_2}}{\mathcal{A}_{S_2}}\int_0^{\infty}\mathbb{P}\Big[SINR_{u_2}^{DL} > \tau_2\Big]r \\ &\quad\times\exp\Big\{-\pi\sum_{j=1}^{2}\lambda_j\Big(\frac{P_j}{P_{S_2}}\Big)^{\zeta_2}r^{\zeta_2}\Big\}dr, \end{aligned} \quad (41)$$

where $\zeta_2 = \frac{2}{\alpha_j/\alpha_2}$.

By setting $Q_2 = I_{u_2}^{UL} + I_{S_2} + I_{S_1}^{DL} + N_0$, we get

$$\begin{aligned}\mathbb{P}\Big[SINR_{u_2}^{DL} > \tau_2\Big] &= \mathbb{P}\Big[h_{S_2,u_2} > {P_{S_2}}^{-1}r^{\alpha_2}\tau_2\ Q_2\Big]\\ &= \int_0^{\infty}\exp\{-r^{\alpha_2}{P_{S_2}}^{-1}\tau_2\ q\}f_{Q_2}(q)dq\\ &= \mathbb{E}_{Q_2}\Big[\exp\{-r^{\alpha_2}{P_{S_2}}^{-1}\tau_2\ q\}\Big]\\ &= \exp\Big\{-r^{\alpha_2}{P_{S_2}}^{-1}N_0\tau_2\Big\}\mathcal{L}_{I_{u_2}^{UL}}(r^{\alpha_2}{P_{S_2}}^{-1}\tau_2)\\ &\quad\times\mathcal{L}_{I_{S_2}}(r^2{P_{S_2}}^{-1}\tau_2)\mathcal{L}_{I_{S_1}^{DL}}(r^{\alpha_2}{P_{S_2}}^{-1}\tau_2). \end{aligned} \quad (42)$$

Following the approach presented in Appendix A, we can obtain the Laplace transforms in (42), starting with the Laplace transform of the interference originated from UL to DL small cell users as follows

$$\mathcal{L}_{I_{u_2}^{UL}}(r^{\alpha_2}{P_{S_2}}^{-1}\tau_2) = \exp\Big\{-\pi r^2\lambda_{u_2}\Big(\frac{P_{u_2}}{P_{S_2}}\Big)^{2/\alpha_2}Y_1(\tau_2,\alpha_2)\Big\} \quad (43)$$

given

$$Y_1(\tau_2,\alpha_2) = \tau_2^{2/\alpha_2}\int_{\tau_2^{-(2/\alpha_2)}}^{\infty}\frac{1}{1+y_1^{\alpha_2/2}}dy_1 = \frac{2\tau_2}{\alpha_2-2}{}_2F_1[1,1-\frac{2}{\alpha_2};2-\frac{2}{\alpha_2};-\tau_2], \quad (44)$$

where $\alpha_2 > 2$, and $y_1 = (r^{\alpha_2}\frac{P_{S_2}}{P_{S_2^*}}\tau_2)^{-2/\alpha_2}r^2$.

Similarly, the second Laplace transform in (42) of the interference originated from small cell BS on DL small cell

user is given as

$$\mathcal{L}_{I_{S_2}}(r^{\alpha_2}{P_{S_2}}^{-1}\tau_2) = \exp\left\{-\pi r^2 \lambda_{S_2}\left(\frac{P_{S_2}}{P_{S_2^*}}\right)^{2/\alpha_2} Y_1(\tau_2,\alpha_2)\right\} \tag{45}$$

The Laplace transform of the interference originated from macrocell BS on DL small cell user is given as

$$\mathcal{L}_{I_{S_1}^{DL}}(r^{\alpha_2}{P_{S_2}}^{-1}\tau_2) = \exp\left\{-\pi\lambda_{S_1}\left(\frac{P_{S_1}}{P_{S_2}}\right)^{2/\alpha_1} \times Y_2(\tau_2,\alpha_1) r^{\frac{2}{\alpha_1/\alpha_2}}\right\}, \tag{46}$$

given

$$Y_2(\tau_2,\alpha_1) = \tau_2^{2/\alpha_1}\int_{{\tau_2}^{-(2/\alpha_1)}}^{\infty}\frac{1}{1+y_2^{\alpha_1/2}}dy_2 = \frac{2\tau_2}{\alpha_1-2}{}_2F_1[1,1-\frac{2}{\alpha_1};2-\frac{2}{\alpha_1};-\tau_2], \tag{47}$$

where $\alpha_1 > 2$, and $y_2 = (r^{\alpha_2}\frac{P_{S_1}}{P_{S_2}}\tau_2)^{-2/\alpha_1} r^2$.

Plugging (43), (45) and (46) into $\mathbb{P}\left[SINR_{u_2}^{DL} > \tau_2\right]$ we obtain

$$\mathbb{P}\left[SINR_{u_2}^{DL} > \tau_2\right] = \exp\left\{-r^{\alpha_2}{P_{S_2}}^{-1}N_0\tau_2 - \pi\left(\left(\eta_1 r^2\right) + \left(\eta_2 r^{\frac{2}{\alpha_2/\alpha_1}}\right) + \left(\eta_3 r^{\frac{2}{\alpha_1/\alpha_2}}\right)\right)\right\}, \tag{48}$$

where

$$\eta_1 = \lambda_{u_2}\left(\frac{P_{u_2}}{P_{S_2}}\right)^{2/\alpha_2} Y_1(\tau_2,\alpha_2)$$
$$\eta_2 = \lambda_{S_2}\left(\frac{P_{S_2}}{P_{S_2^*}}\right)^{2/\alpha_2} Y_1(\tau_2,\alpha_2)$$
$$\eta_3 = \lambda_{S_1}\left(\frac{P_{S_1}}{P_{S_2}}\right)^{2/\alpha_1} Y_2(\tau_2,\alpha_1).$$

Similarly, the analysis of the second term in (40) of the outage probability during ABS subframes transmission is given as follows.

First, we consider the SINR expressed in (6) for the ABS subframes transmission. By setting $Q_2^* = I_{u_2}^{UL} + I_{S_2} + N_0$, we have

$$\begin{aligned}
&\mathbb{P}\left[SINR_{u_2}^{DL_ABS} > \tau_2\right] \\
&= \mathbb{P}\left[h_{S_2,u_2} > {P_{S_2}}^{-1} r^{\alpha_2}\tau_2\, Q_2^*\right] \\
&= \int_0^{\infty}\exp\{-r^{\alpha_2}{P_{S_2}}^{-1}\tau_2\, q\} f_{Q_2^*}(q)dq \\
&= \mathbb{E}_{Q_2^*}\left[\exp\{-r^{\alpha_2}{P_{S_2}}^{-1}\tau_2\, q\}\right] \\
&= \exp\left\{-r^{\alpha_2}{P_{S_2}}^{-1}N_0\tau_2\right\}\mathcal{L}_{I_{u_2}^{UL}}(r^{\alpha_2}{P_{S_2}}^{-1}\tau_2) \\
&\quad\times\mathcal{L}_{I_{S_2}}(r^{\alpha_2}{P_{S_2}}^{-1}\tau_2).
\end{aligned} \tag{49}$$

Since we have previously derived $\mathcal{L}_{I_{u_2}^{UL}}(r^{\alpha_2}{P_{S_2}}^{-1}\tau_2)$ and $\mathcal{L}_{I_{S_2}}(r^{\alpha_2}{P_{S_2}}^{-1}\tau_2)$, we can obtain the probability $\mathbb{P}\left[SINR_{u_2}^{DL\_ABS} > \tau_2\right]$ as

$$\mathbb{P}\left[SINR_{u_2}^{DL\_ABS} > \tau_2\right] = \exp\left\{-r^{\alpha_2}{P_{S_2}}^{-1}N_0\tau_2 - \pi\left(\left(\eta_1 r^2\right) + \left(\eta_2 r^{\frac{2}{\alpha_2/\alpha_1}}\right)\right)\right\}. \tag{50}$$

Therefore, the final expression for the outage probability for a randomly located DL small cell user, considering eICIC is given in (11).

C. PROOF OF THEOREM 3

From (10), The outage probability $\mathbb{O}_2^{UL}$ can be obtained by

$$\mathbb{O}_2^{UL} = (1-\rho)\mathbb{E}\left[\mathbb{P}\left[SINR_{S_2}^{UL} < \tau_3\right]\right] + \rho\mathbb{E}\left[\mathbb{P}\left[SINR_{S_2}^{UL\_ABS} < \tau_3\right]\right] \tag{51}$$

Starting by the first term of (51), we have

$$\begin{aligned}
&(1-\rho)\mathbb{E}\left[\mathbb{P}\left[SINR_{S_2}^{UL} > \tau_2\right]\right] \\
&= 1 - \left((1-\rho)\int_0^{\infty}\mathbb{P}\left[SINR_{S_2}^{UL} > \tau_2\right] f_{R_{S_2,u_2^{UL}}}(r)dr\right) \\
&= 1 - \left(2\pi\,(1-\rho)\lambda_{S_2}\int_0^{\infty}\mathbb{P}\left[SINR_{S_2}^{UL} > \tau_2\right] r \times \exp\left\{-\pi\lambda_2 r^2\right\}dr\right),
\end{aligned} \tag{52}$$

Following the same steps used in previous derivations, taking into account the power control factor ϵ, we obtain the final expression of the UL small cell outage probability as given in (12).

REFERENCES

[1] A. Gohil, H. Modi, and S. K. Patel, "5G technology of mobile communication: A survey," in *Proc. IEEE ISS*, Mar. 2013, pp. 288–292.
[2] M. Duarte, C. Dick, and A. Sabharwal, "Experiment-driven characterization of full-duplex wireless systems," *IEEE Trans. Wireless Commun.*, vol. 11, no. 12, pp. 4296–4307, Dec. 2012.
[3] D. Bharadia, E. McMilin, and S. Katti, "Full duplex radios," *SIGCOMM Comput. Commun. Rev.*, vol. 43, no. 4, pp. 375–386, Aug. 2013.
[4] M. Duarte *et al.*, "Design and characterization of a full-duplex multiantenna system for WiFi networks," *IEEE Trans. Veh. Technol.*, vol. 63, no. 3, pp. 1160–1177, Mar. 2014.
[5] H. Ju, X. Shang, H. V. Poor, and D. Hong, "Rate improvement of beamforming systems via bi-directional use of spatial resources," in *Proc. IEEE GLOBECOM*, Dec. 2011, pp. 1–5.
[6] B. P. Day, A. R. Margetts, D. W. Bliss, and P. Schniter, "Full-duplex MIMO relaying: Achievable rates under limited dynamic range," *IEEE J. Sel. Areas Commun.*, vol. 30, no. 8, pp. 1541–1553, Sep. 2012.
[7] C. Cox and E. Ackerman, "Demonstration of a single-aperture, full-duplex communication system," in *Proc. IEEE RWS*, Jan. 2013, pp. 148–150.
[8] M. E. Knox, "Single antenna full duplex communications using a common carrier," in *Proc. IEEE WAMICON*, Apr. 2012, pp. 1–6.
[9] H. Ju, X. Shang, H. V. Poor, and D. Hong, "Bi-directional use of spatial resources and effects of spatial correlation," *IEEE Trans. Wireless Commun.*, vol. 10, no. 10, pp. 3368–3379, Oct. 2011.
[10] M. O. Al-Kadri, A. Aijaz, and A. Nallanathan, "Ergodic capacity of interference coordinated HetNet with full-duplex small cells," in *Proc. EW*, May 2015, pp. 1–6.
[11] D. Kim, S. Park, H. Ju, and D. Hong, "Transmission capacity of full-duplex-based two-way ad hoc networks with ARQ protocol," *IEEE Trans. Veh. Technol.*, vol. 63, no. 7, pp. 3167–3183, Sep. 2014.

[12] H. Ju, E. Oh, and D. Hong, "Catching resource-devouring worms in next-generation wireless relay systems: Two-way relay and full-duplex relay," *IEEE Commun. Mag.*, vol. 47, no. 9, pp. 58–65, Sep. 2009.

[13] G. Zheng, I. Krikidis, J. Li, A. P. Petropulu, and B. Ottersten, "Improving physical layer secrecy using full-duplex jamming receivers," *IEEE Trans. Signal Process.*, vol. 61, no. 20, pp. 4962–4974, Oct. 2013.

[14] M. O. Al-Kadri, A. Aijaz, and A. Nallanathan, "An energy-efficient full-duplex MAC protocol for distributed wireless networks," *IEEE Wireless Commun. Lett.*, vol. 5, no. 1, pp. 44–47, Feb. 2016.

[15] J. G. Andrews, "Seven ways that HetNets are a cellular paradigm shift," *IEEE Commun. Mag.*, vol. 51, no. 3, pp. 136–144, Mar. 2013.

[16] V. Chandrasekhar, J. G. Andrews, and A. Gatherer, "Femtocell networks: A survey," *IEEE Commun. Mag.*, vol. 46, no. 9, pp. 59–67, Sep. 2008.

[17] *Summary of the Description of Candidate eICIC Solutions*, document R1-104968, 3GPP, Madrid, Spain, Aug. 2010.

[18] M. Z. Win, P. C. Pinto, and L. A. Shepp, "A mathematical theory of network interference and its applications," *Proc. IEEE*, vol. 97, no. 2, pp. 205–230, Feb. 2009.

[19] H. Elsawy, E. Hossain, and M. Haenggi, "Stochastic geometry for modeling, analysis, and design of multi-tier and cognitive cellular wireless networks: A survey," *IEEE Commun. Surveys Tuts.*, vol. 15, no. 3, pp. 996–1019, 3rd Quart., 2013.

[20] R. W. Heath, M. Kountouris, and T. Bai, "Modeling heterogeneous network interference using Poisson point processes," *IEEE Trans. Signal Process.*, vol. 61, no. 16, pp. 4114–4126, Aug. 2013.

[21] U. Schilcher, S. Toumpis, M. Haenggi, A. Crismani, G. Brandner, and C. Bettstetter, "Interference functionals in Poisson networks," *IEEE Trans. Inf. Theory*, vol. 62, no. 1, pp. 370–383, Jan. 2016.

[22] H. S. Dhillon, R. K. Ganti, F. Baccelli, and J. G. Andrews, "Modeling and analysis of K-tier downlink heterogeneous cellular networks," *IEEE J. Sel. Areas Commun.*, vol. 30, no. 3, pp. 550–560, Apr. 2012.

[23] T. D. Novlan, H. S. Dhillon, and J. G. Andrews, "Analytical modeling of uplink cellular networks," *IEEE Trans. Wireless Commun.*, vol. 12, no. 6, pp. 2669–2679, Jun. 2013.

[24] H. S. Dhillon, R. K. Ganti, and J. G. Andrews, "Load-aware modeling and analysis of heterogeneous cellular networks," *IEEE Trans. Wireless Commun.*, vol. 12, no. 4, pp. 1666–1677, Apr. 2013.

[25] Y. S. Soh, T. Q. S. Quek, M. Kountouris, and H. Shin, "Energy efficient heterogeneous cellular networks," *IEEE J. Sel. Areas Commun.*, vol. 31, no. 5, pp. 840–850, May 2013.

[26] H.-S. Jo, Y. J. Sang, P. Xia, and J. G. Andrews, "Heterogeneous cellular networks with flexible cell association: A comprehensive downlink SINR analysis," *IEEE Trans. Wireless Commun.*, vol. 11, no. 10, pp. 3484–3495, Oct. 2012.

[27] D. Kim, H. Lee, and D. Hong, "A survey of in-band full-duplex transmission: From the perspective of PHY and MAC layers," *IEEE Commun. Surveys Tuts.*, vol. 17, no. 4, pp. 2017–2046, 4th Quart., 2015.

[28] J. Lee and T. Q. S. Quek, "Hybrid full-/half-duplex system analysis in heterogeneous wireless networks," *IEEE Trans. Wireless Commun.*, vol. 14, no. 5, pp. 2883–2895, May 2015.

[29] H. Tabassum, A. H. Sakr, and E. Hossain, "Massive MIMO-enabled wireless backhauls for full-duplex small cells," in *Proc. IEEE GLOBECOM*, Dec. 2015, pp. 1–6.

[30] S. Han, C. Yang, and P. Chen, "Full duplex-assisted intercell interference cancellation in heterogeneous networks," *IEEE Trans. Commun.*, vol. 63, no. 12, pp. 5218–5234, Dec. 2015.

[31] A. AlAmmouri, H. ElSawy, and M.-S. Alouini, "Flexible design for α-duplex communications in multi-tier cellular networks," *IEEE Trans. Commun.*, vol. 64, no. 8, pp. 3548–3562, Aug. 2016.

[32] S. Goyal, C. Galiotto, N. Marchetti, and S. Panwar, "Throughput and coverage for a mixed full and half duplex small cell network," in *Proc. IEEE ICC*, May 2016, pp. 1–7.

[33] S. Singh, H. S. Dhillon, and J. G. Andrews, "Offloading in heterogeneous networks: Modeling, analysis, and design insights," *IEEE Trans. Wireless Commun.*, vol. 12, no. 5, pp. 2484–2497, May 2013.

[34] D. W. K. Ng, E. S. Lo, and R. Schober, "Dynamic resource allocation in MIMO-OFDMA systems with full-duplex and hybrid relaying," *IEEE Trans. Commun.*, vol. 60, no. 5, pp. 1291–1304, May 2012.

[35] T. Riihonen, S. Werner, and R. Wichman, "Mitigation of loopback self-interference in full-duplex MIMO relays," *IEEE Trans. Signal Process.*, vol. 59, no. 12, pp. 5983–5993, Dec. 2011.

[36] D. Kim, H. Ju, S. Park, and D. Hong, "Effects of channel estimation error on full-duplex two-way networks," *IEEE Trans. Veh. Technol.*, vol. 62, no. 9, pp. 4666–4672, Nov. 2013.

[37] J. I. Choi, M. Jain, K. Srinivasan, P. Levis, and S. Katti, "Achieving single channel, full duplex wireless communication," in *Proc. ACM MobiCom*, Sep. 2010, pp. 1–12.

[38] M. Jain *et al.*, "Practical, real-time, full duplex wireless," in *Proc. ACM MobiCom*, Nov. 2011, pp. 301–312.

[39] T. Snow, C. Fulton, and W. J. Chappell, "Transmit–receive duplexing using digital beamforming system to cancel self-interference," *IEEE Trans. Microw. Theory Techn.*, vol. 59, no. 12, pp. 3494–3503, Dec. 2011.

[40] P. Lioliou, M. Viberg, M. Coldrey, and F. Athley, "Self-interference suppression in full-duplex MIMO relays," in *Proc. IEEE ASILOMAR*, Nov. 2010, pp. 658–662.

[41] J. G. Andrews, F. Baccelli, and R. K. Ganti, "A tractable approach to coverage and rate in cellular networks," *IEEE Trans. Commun.*, vol. 59, no. 11, pp. 3122–3134, Nov. 2011.

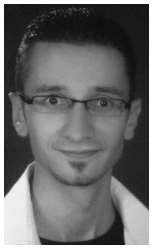

MHD OMAR AL-KADRI (S'12) received the B.Eng. degree from IUST, Syria, in 2010, and the M.Sc. degree (Hons.) in networking and data communication from Kingston University. He is currently pursuing the Ph.D. degree in networks and telecommunication engineering with King's College London. His research interests include full-duplex technology, HetNet, wireless communications, computer networks, networks security, and protocols of MAC and network layers.

YANSHA DENG (S'13–M'16) received the Ph.D. degree in electrical engineering from the Queen Mary University of London, U.K., in 2015. She is currently a Post-Doctoral Research Fellow with the Department of Informatics, King's College London, U.K. Her research interests include massive MIMO, HetNets, molecular communication, cognitive radio, cooperative networks, and physical layer security. She received the Best Paper Award from ICC 2016. She has served as a TPC member for many IEEE conferences, such as IEEE GLOBECOM and ICC.

ADNAN AIJAZ (M'14) received the B.E. degree in electrical (telecom) engineering from the National University of Sciences and Technology, Pakistan, and the Ph.D. degree in telecommunications engineering from King's College London (KCL), in 2014. He was with cellular industry for nearly 2.5 years in the areas of network performance management, optimization, and quality assurance. He held a post-doctoral position at KCL for one year. He moved to Toshiba Research Europe Ltd., where he is currently a Senior Research Engineer. His primary research focus is on wireless networking, with an emphasis on 5G cellular networks, cognitive radio networks, sensor networks, 802.11-based WLANs, Internet-of-Things, and, tactile Internet. His publications in these areas have been featured in internationally renowned conferences and journals.

ARUMUGAM NALLANATHAN (S'97–M'00–SM'05–F'16) served as the Head of Graduate Studies at the School of Natural and Mathematical Sciences, King's College London, from 2011 to 2012. He was an Assistant Professor in the Department of Electrical and Computer Engineering, National University of Singapore, from 2000 to 2007. He is currently a Professor of Wireless Communications with the Department of Informatics, King's College London. He has authored over 300 technical papers in scientific journals and international conferences. His research interests include 5G wireless networks, molecular communications, energy harvesting, and cognitive radio networks. He was a co-recipient of the Best Paper Award presented at the IEEE International Conference on Communications in 2016 and the IEEE International Conference on Ultra-Wideband in 2007. He is an IEEE Distinguished Lecturer.

Dr. Nallanathan received the IEEE Communications Society SPCE Outstanding Service Award in 2012 and the IEEE Communications Society RCC Outstanding Service Award in 2014. He served as the Chair of the Signal Processing and Communication Electronics Technical Committee of the IEEE Communications Society, the Technical Program Co-Chair (MAC track) of IEEE WCNC 2014, the Co-Chair of IEEE GLOBECOM 2013 (Communications Theory Symposium), the Co-Chair of IEEE ICC 2012 (Signal Processing for Communications Symposium), the Co-Chair of IEEE GLOBECOM 2011 (Signal Processing for Communications Symposium), the Technical Program Co-Chair of the IEEE International Conference on UWB 2011, the Co-Chair of IEEE ICC 2009 (Wireless Communications Symposium), the Co-Chair of IEEE GLOBECOM 2008 (Signal Processing for Communications Symposium), and the General Track Chair of IEEE VTC 2008. He was an Editor of the IEEE TRANSACTIONS ON WIRELESS COMMUNICATIONS from 2006 to 2011, IEEE WIRELESS COMMUNICATIONS LETTERS, and IEEE SIGNAL PROCESSING LETTERS. He is an Editor of the IEEE TRANSACTIONS ON COMMUNICATIONS and the IEEE TRANSACTIONS ON VEHICULAR TECHNOLOGY.